Electron Paramagnetic Resonance Dynamic Signatures of TAR RNA−Small Molecule Complexes Provide Insight into RNA Structure and Recognition†

Thomas E. Edwards and Snorri Th. Sigurdsson*

Department of Chemistry, University of Washington, Seattle, Washington 98195-1700

Received June 13, 2002; Revised Manuscript Received September 20, 2002

ABSTRACT: Electron paramagnetic resonance (EPR) spectroscopy was utilized to investigate the correlation between RNA structure and RNA internal dynamics in complexes of HIV-1 TAR RNA with small molecules. TAR RNAs containing single nitroxide spin-labels in the 2′-position of U23, U25, U38, or U40 were incubated with compounds known to inhibit TAR−Tat complex formation. The combined changes in nucleotide mobility at all four sites, as monitored by their EPR spectral width, yield a dynamic signature for each compound. The multicyclic dyes Hoechst 33258, DAPI, and berenil bind to TAR RNA in a similar manner and gave nearly identical signatures. Different signatures were obtained for the acridine derivative CGP 40336A and the aminoglycoside antibiotic neomycin, which bind to different regions of the RNA. The dynamic signature for guanidinoneomycin was remarkably similar to that obtained for argininamide and is evidence for guanidinoneomycin binding to the same site as arginine 52 of the Tat protein, rather than to the neomycin binding site. The data presented here show that the dynamic signatures provide strong insights into RNA structure and recognition and demonstrate the value of EPR spectroscopy for the investigation of small molecule binding to RNA.

RNA performs numerous roles in essential cellular functions, thus making it an important target for drug discovery (*1*, *2*). In addition, targeting RNA and RNA−protein interactions is an important strategy for antiviral therapy. One such target is the human immunodeficiency virus (HIV)[1] trans activation responsive (TAR) RNA (Figure 1A) whose binding to the Tat protein is essential for production of full-length RNA transcripts during viral replication (*3*, *4*). Small molecules that disrupt this interaction have been shown to display antiviral activity in vitro (*5*).

High-resolution structural data, obtained by X-ray crystallography or NMR spectroscopy, are the most useful information for studying RNA and its complexes with proteins or small molecules. Despite recent advances in the study of antibiotic binding to bacterial ribosomes by X-ray crystallography (*6*−*8*), RNA−inhibitor studies frequently rely on techniques that give low-resolution structural information, such as chemical and enzymatic footprinting, in which binding sites are inferred from changes in RNA cleavage rates upon addition of small molecules (*9*−*14*). A potential disadvantage of these approaches is that a ligand-induced conformational change may affect the rates of RNA cleavage distal to the binding site. Circular dichroism can distinguish between RNA groove binding and intercalation but cannot identify individual binding sites (*15*). Other techniques that

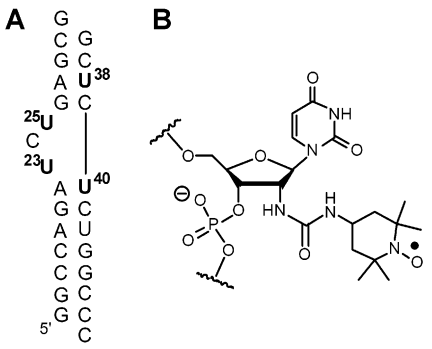

FIGURE 1: (A) TAR RNA construct used in this study. Spin-labeled nucleotides are shown in bold. (B) Nitroxide spin-label covalently linked to the 2′-position of a uridine nucleotide in RNA.

are valuable for determining noncovalent binding of small molecules to RNA, such as mass spectrometry (*16*), fluorescence (*17*), and surface plasmon resonance (*18*, *19*), yield binding constants but do not give structural information.

Electron paramagnetic resonance (EPR) spectroscopy has been used extensively in the study of protein structure and function (*20*, *21*). For the study of RNA by EPR, we have utilized the selective reaction of 2′-amino groups with isocyanates to introduce nitroxide radicals, commonly used reporter groups for EPR studies, into internal, base-paired sites of RNA (Figure 1B) (*22*). The motions of the nitroxide were shown to be strongly coupled to the motions of the spin-labeled nucleotide, enabling identification of nucleotides in different structural contexts by EPR spectroscopy. More recently, we determined the change in dynamics of four specific nucleotides (U23, U25, U38, and U40) in the TAR RNA (Figure 1A) upon binding to metal ions and Tat protein derivatives (*23*). Plotting the change in RNA dynamics as a

† This work was supported by the National Institutes of Health (Grants GM56947 and GM62360) and an NIH National Research Service award (5 T32 GM08268) to T.E.E.

* Corresponding author. E-mail: sigurdsson@chem.washington.edu. Tel: +1-206-616-8276. Fax: +1-206-685-8665.

[1] Abbreviations: HIV, human immunodeficiency virus; TAR, trans activation responsive region; Tat, trans activator of transcription; EPR, electron paramagnetic resonance; CW-EPR, continuous wave EPR; ELD, electric linear dichroism; UV, ultraviolet; CD, circular dichroism.

10.1021/bi026299a CCC: $22.00
Published on Web 11/20/2002

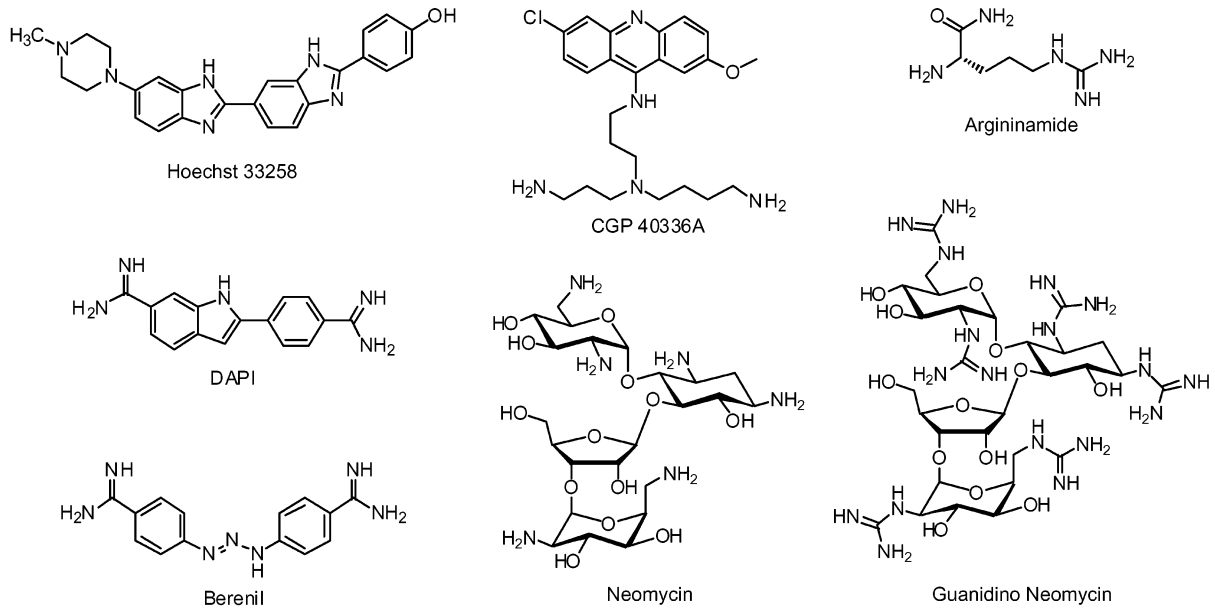

FIGURE 2: Structures and names of the compounds used in this study.

function of nucleotide position yielded a dynamic signature, characteristic for the molecule or ion being studied.

In this report we provide additional evidence for a strong correlation between RNA internal dynamics and structure. Several different compounds that have been shown to inhibit the TAR−Tat complex formation (Figure 2) were incubated with spin-labeled TAR RNAs and their EPR dynamic signatures determined. Compounds that bind differently to the RNA give different signatures whereas compounds that bind in a similar manner yield nearly identical signatures. Furthermore, our data indicate that a guanidino derivative of neomycin binds to the same site as argininamide, rather than the neomycin binding site. Thus, EPR dynamic signatures not only give information about RNA dynamics but also provide insights into RNA structure and binding, illustrating that EPR is a valuable technique for studying the interactions of small molecules with RNA.

MATERIALS AND METHODS

Materials. Hoechst 33258 [2′-(4-hydroxyphenyl)-5-(4-methyl-1-piperazinyl)-2,5′-bis(1*H*-benzimidazole)], berenil [1,3-bis(4-phenylamidinium)triazene], and DAPI (4′,6-diamidino-2-phenylindole) were purchased from Sigma. Neomycin sulfate was obtained from ICN Biomedicals (Aurora, OH). Guanidinoneomycin and CGP 40336A were generously donated by Profs. M. Goodman and Y. Tor (University of California, San Diego) and Novartis Pharma (Basel, Switzerland), respectively. 2′-Amino-containing oligoribonucleotides (Dharmacon Research Inc.) were spin-labeled using 4-isocyanato-TEMPO, purified, and quantified as previously described (*22*, *23*).

EPR Spectroscopy. RNA samples (2.0 nmol in 7.0 μL of 20% aqueous sucrose/100 mM NaCl, 10 mM sodium phosphate, and 0.1 mM Na_2EDTA, pH 7.0) were annealed on a thermocycler using the following stepwise heating and cooling protocol: 90 °C for 2 min, 60 °C for 5 min, 50 °C for 5 min, 40 °C for 5 min, and 25 °C for 15 min. Solutions of small molecule inhibitors (3.0 μL in the aqueous sucrose buffer) were added and thoroughly mixed (final inhibitor concentrations ranged from 0.2 to 5 mM). CW-EPR spectra were acquired on a Bruker EMX 300 spectrometer (9.34 GHz) with a TE102 cavity at 0 °C (±0.2 °C) using 200 μM RNA samples in 0.8 × 1.0 mm quartz capillaries (VitroCom). Spectra were collected with 8 mW power, 100 kHz modulation frequency, 1.0 G modulation amplitude, 42 s sweep time, and typically 100 scans. EPR spectra were subsequently analyzed using WIN-EPR and Matlab as previously described (*23*).

RESULTS

Multicyclic Dyes. To determine the concentration dependence of the dyes on the EPR spectra, we incubated the dyes at 0−5 mM concentration with spin-labeled TAR RNAs (0.2 mM). The changes in U23 for Hoechst 33258 are illustrative (Figure 3), in which the spectral width decreased, indicative of an increase in nucleotide mobility, up to a concentration of 0.2 mM (1 equiv). Further addition of the dye resulted in virtually no changes until a concentration of 3 mM was reached. Above 3 mM concentration, large increases in spectral width were observed for U23, U25, U38, and U40. Similar results were also obtained for the other dyes. A construct of the TAR RNA lacking the trinucleotide bulge (*22*) also showed a dramatic decrease in mobility of U40 in the presence of 5 mM Hoechst 33258 (data not shown). Taken together, these results indicate that nonspecific binding occurs at the higher concentrations. Therefore, the data reported here were obtained at a concentration of 0.5 mM.

The change in spectral width was plotted as a function of nucleotide position to give dynamic signatures (*23*) for Hoechst 33258, DAPI, and berenil (Figure 4). All of these dyes have the same dynamic signature with an increase in mobility at U23, U25, and U38 while the mobility of U40 decreased. The only observed differences between the dyes were some variations in the degree of change observed, most notably in the presence of berenil at positions U25 and U40.

CGP 40336A. The acridine derivative CGP 40336A, developed by Novartis, is the tightest known inhibitor of the TAR−Tat interaction (CD_{50} 22 nM) and appears to bind

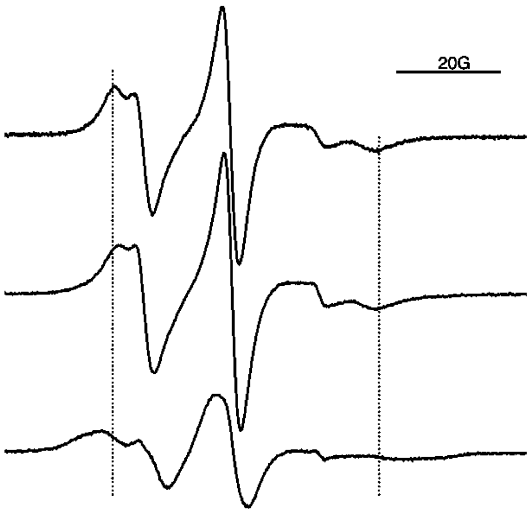

FIGURE 3: Effect of Hoechst 33258 on the EPR spectra of U23 spin-labeled TAR RNA. The spectra were recorded in the absence of dye (top) and at 0.5 mM (middle) and 5 mM (bottom) dye concentrations. The vertical lines show the spectral width for the unbound RNA (top), illustrating that the spectral width decreases at low concentrations but increases dramatically at higher concentrations.

selectively to the G26·C39 base pair, while stacking between A22 and U23 (*13*, *24*). At 0.5 mM concentration, the mobility of U23 and U40 decreased with an increase in mobility for U25 and U38, resulting in a unique dynamic signature for this compound (Figure 4).

Neomycin and Guanidinoneomycin. In the presence of 0.4 mM neomycin, a decrease in mobility was observed at positions U23, U25, U38, and U40, giving a dynamic signature which is different from the other compounds (Figure 4). At this concentration, neomycin should predominantly form a 1:1 complex with the RNA (*25*). A further decrease in mobility for U23 upon addition of neomycin was observed up to 2 mM (10 equiv), after which no additional change was detected by EPR (up to 10 mM; data not shown). Multiple drug binding has previously been observed by gel shift assays (*26*).

Guanidinoneomycin, a neomycin analogue where the amino groups of neomycin have been converted to guanidino groups (*27*), gave a dynamic signature different from that of neomycin (Figure 4). The mobility of U23, U38, and U40 decreased while U25 became more mobile, resulting in a dynamic signature similar to that previously obtained for argininamide (*23*), which has been observed to bind TAR through its guanidino group (*28*, *29*).

DISCUSSION

Our previous studies on RNA dynamics using EPR spectroscopy have indicated a correlation between RNA structure and dynamics. For example, calcium and sodium ions had similar effects on the internal dynamics of the TAR RNA, which were distinctively different than the effects induced by derivatives of the Tat protein (*23*). The main goal of this study was to determine if the correlation between RNA dynamics and structure previously observed is a general theme by monitoring the change in RNA internal dynamics upon addition of small molecule inhibitors (Figure 2) of the TAR−Tat interaction. We show here that molecules that bind in like fashion cause similar changes in RNA dynamics, indicating that RNA structure and dynamics are indeed strongly correlated.

The changes in EPR spectral width were plotted as a function of nucleotide position to yield a dynamic signature for each compound (Figure 4). The strength of this approach lies in the selection of a sufficient number of spin-labeled sites to give a unique signature for each compound, which reduces the analysis of individual EPR spectra to a simple measurement of the spectral width. A decrease in nucleotide mobility is concomitant with an increase in spectral width, whereas a narrower spectrum indicates an increase in mobility (*30*). Compounds that bind to different regions of the RNA (Figure 5) yield different dynamic signatures. On the other hand, structurally related compounds, such as the multicyclic dyes Hoechst 33258, DAPI, and berenil, have nearly identical dynamic signatures, indicating that they bind in a manner similar to that of the RNA. Electric linear

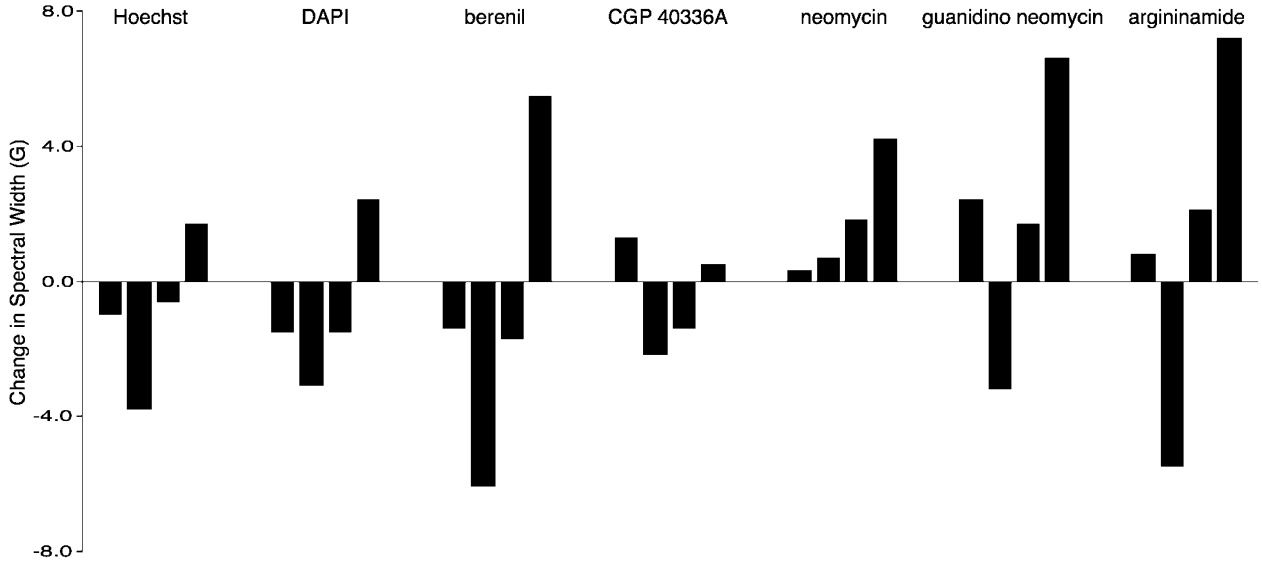

FIGURE 4: Dynamic signatures of TAR RNA inhibitor complexes. The change in spectral width is plotted as a function of nucleotide position (U23, U25, U38, and U40) for each compound. An increase in spectral width corresponds to a decrease in nucleotide mobility and vice versa.

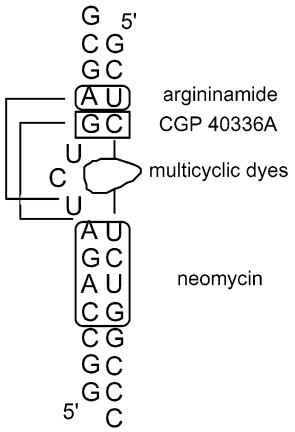

FIGURE 5: Schematic representation of the TAR RNA binding sites for the compounds used in this study. Argininamide binds to the upper duplex while inducing a U23·A27·U38 base triple formation. CGP 40336A stacks between A22 and U23 while specifically recognizing the Hoogsteen face of the G26·C39 base pair. The multicyclic dyes Hoechst 33258, DAPI, and berenil bind RNA in a pocket created by the trinucleotide bulge, while neomycin binds to the lower stem.

dichroism (ELD) (*31*), UV and CD spectroscopy, thermal denaturation, and nuclease footprinting experiments (*11*) have provided evidence that the dyes all bind to the major groove pocket created by the trinucleotide bulge. Although all three compounds bind to the same site, the ELD measurements suggested that berenil bound slightly differently through a combination of intercalation and groove binding (*31*). Berenil had a significantly larger effect on the mobility of U25 and U40 than DAPI and Hoechst 33258, providing further evidence that berenil may bind with a slightly different geometry.

The acridine−spermidine conjugate CGP 40336A is the tightest binding TAR inhibitor known (CD_{50} 22 nM) and is a potent antiviral agent in vitro (*24*). This compound appears to bind selectively to the G26·C39 base pair with minimal reorganization of the RNA structure (*13*, *24*). Consistent with this observation, we find the least amount of change in RNA dynamics for CGP 40336A, which is a clear indication that tight binding at a specific site does not necessarily correlate with an overall decrease in RNA mobility. The dynamic signature of this compound is also different from all the others, with a decrease in the mobility of U23 and U40 and an increase in mobility at U25 and U38 (Figure 4).

The aminoglycoside antibiotic neomycin inhibits TAR−Tat formation through an allosteric mechanism as evidenced by kinetic studies, enzymatic footprinting, and circular dichroism spectroscopy (*32*). These experiments suggested that the binding site is in the minor groove of the lower stem, immediately below the trinucleotide bulge, and further supported by solution NMR data (*25*). Molecular simulations have also predicted binding of neomycin to the lower stem, but in the major rather than the minor groove (*33*). The dynamic signature for neomycin shows a unique pattern, with all four nucleotides becoming less mobile (Figure 4).

The aminoglycoside conjugate guanidinoneomycin, where the amino groups of neomycin have been converted to guanidino groups, was designed to utilize the binding properties of both neomycin and the guanidino groups found in the arginine-rich basic region of the Tat protein (*27*, *34*). The dynamic signatures for guanidinoneomycin and argininamide (*23*), the simplest Tat derivative, are strikingly similar, with U23, U38, and U40 becoming less mobile and U25 increasing in mobility (Figure 4). In contrast, the mobility of U25 is reduced for neomycin. These data are consistent with guanidinoneomycin binding to the same site as arginine 52 of the Tat protein, causing the trinucleotide bulge to invert and U23 forming a triple base pair with U38 and A27 (*29*, *35*, *36*). However, confirmation of this EPR-based hypothesis requires a high-resolution structure of guanidinoneomycin bound to the TAR RNA.

The data presented here show that the flexibility of RNA is reduced upon binding small molecules, which has also been observed for RNA aptamers that have been selected to bind small molecules (*37*). This result corroborates the notion of "induced fit" that has been observed in RNA−protein (*38*, *39*) and RNA−peptide binding (*23*). However, an overall increase in the mobility of the RNA is observed for the dyes: only U40 at the intersection of the two helices becomes more rigid. Knowledge about RNA dynamics at the nucleotide level is scarce (*22*, *23*, *40*, *41*), but as more information becomes available, it will be possible to better dissect the interplay between RNA structure and dynamics. Such analysis will increase our understanding of the role dynamics play in RNA function and aid in the difficult task of designing small molecules that bind flexible RNA receptor sites and thereby inhibit biological function.

ACKNOWLEDGMENT

We thank Dr. T. M. Okonogi for technical assistance, Prof. B. Robinson and Prof. G. Varani for many helpful discussions, Prof. M. Goodman, Prof. Y. Tor, and N. W. Luedtke for the generous gift of guanidinoneomycin, and Novartis Pharma Inc. for CGP 40336A. We acknowledge the use of an EPR spectrometer obtained through a center grant from the NIH (P30 ES07033).

SUPPORTING INFORMATION AVAILABLE

Eight figures showing EPR spectra of TAR RNA−small molecule complexes and dynamic signatures of Hoechst 33258. This material is available free of charge via the Internet at http://pubs.acs.org.

REFERENCES

1. Chow, C. S., and Bogdan, F. M. (1997) *Chem. Rev. 97*, 1489−1513.
2. Gallego, J., and Varani, G. (2001) *Acc. Chem. Res. 34*, 836−843.
3. Frankel, A. D. (1992) *Curr. Opin. Genet. Dev. 2*, 293−298.
4. Jones, K. A., and Peterlin, B. M. (1994) *Annu. Rev. Biochem. 63*, 717−743.
5. Litovchick, A., Evdokimov, A. G., and Lapidot, A. (2000) *Biochemistry 39*, 2838−2852.
6. Brodersen, D. E., Clemons, W. M., Jr., Carter, A. P., Morgan-Warren, R. J., Wimberly, B. T., and Ramakrishnan, V. (2000) *Cell 103*, 1143−1154.
7. Carter, A. P., Clemons, W. M., Brodersen, D. E., Morgan-Warren, R. J., Wimberly, B. T., and Ramakrishnan, V. (2000) *Nature 407*, 340−348.
8. Schlunzen, F., Zarivach, R., Harms, J., Bashan, A., Tocilj, A., Albrecht, R., Yonath, A., and Franceschi, F. (2001) *Nature 413*, 814−821.
9. Rosendahl, G., and Douthwaite, S. (1994) *Nucleic Acids Res. 22*, 357−363.
10. Recht, M. I., Fourmy, D., Blanchard, S. C., Dahlquist, K. D., and Puglisi, J. D. (1996) *J. Mol. Biol. 262*, 421−436.
11. Dassonneville, L., Hamy, F., Colson, P., Houssier, C., and Bailly, C. (1997) *Nucleic Acids Res. 25*, 4487−4492.

12. Gelus, N., Bailly, C., Hamy, F., Klimkait, T., Wilson, W. D., and Boykin, D. W. (1999) *Bioorg. Med. Chem. 7*, 1089−1096.
13. Gelus, N., Hamy, F., and Bailly, C. (1999) *Bioorg. Med. Chem. 7*, 1075−1079.
14. McPike, M. P., Goodisman, J., and Dabrowiak, J. C. (2001) *Methods Enzymol. 340*, 431−449.
15. Eriksson, M., and Norden, B. (2001) *Methods Enzymol. 340*, 68−98.
16. Hofstadler, S. A., and Griffey, R. H. (2001) *Chem. Rev. 101*, 377−390.
17. Luedtke, N. W., and Tor, Y. (2000) *Angew. Chem., Int. Ed. 39*, 1788−1790.
18. Hendrix, M., Priestley, E. S., Joyce, G. F., and Wong, C. H. (1997) *J. Am. Chem. Soc. 119*, 3641−3648.
19. Davis, T. M., and Wilson, W. D. (2001) *Methods Enzymol. 340*, 22−51.
20. Hubbell, W. L., and Altenbach, C. (1994) *Curr. Opin. Struct. Biol. 4*, 566−573.
21. Hubbell, W. L., Gross, A., Langen, R., and Lietzow, M. A. (1998) *Curr. Opin. Struct. Biol. 8*, 649−656.
22. Edwards, T. E., Okonogi, T. M., Robinson, B. H., and Sigurdsson, S. T. (2001) *J. Am. Chem. Soc. 123*, 1527−1528.
23. Edwards, T. E., Okonogi, T. M., and Sigurdsson, S. T. (2002) *Chem. Biol. 9*, 699−706.
24. Hamy, F., Brondani, V., Florsheimer, A., Stark, W., Blommers, M. J. J., and Klimkait, T. (1998) *Biochemistry 37*, 5086−8095.
25. Faber, C., Sticht, H., Schweimer, K., and Rösch, P. (2000) *J. Biol. Chem. 275*, 20660−20666.
26. Mei, H. Y., Mack, D. P., Galan, A. A., Halim, N. S., Heldsinger, A., Loo, J. A., Moreland, D. W., Sannes-Lowery, K. A., Sharmeen, L., Truong, H. N., and Czarnik, A. W. (1997) *Bioorg. Med. Chem. 5*, 1173−1184.
27. Baker, T. J., Luedtke, N. W., Tor, Y., and Goodman, M. (2000) *J. Org. Chem. 65*, 9054−9058.
28. Calnon, B. J., Tidor, B., Biancalana, S., Hudson, D., and Frankel, A. D. (1991) *Science 252*, 1167−1171.
29. Brodsky, A. S., and Williamson, J. R. (1997) *J. Mol. Biol. 267*, 624−639.
30. Berliner, L. J., Ed. (1976) *Spin Labeling: Theory and Applications*, Academic Press, New York.
31. Bailly, C., Colson, P., Houssier, C., and Hamy, F. (1996) *Nucleic Acids Res. 24*, 1460−1464.
32. Wang, S., Huber, P. W., Mei, C., Czarnik, A. W., and Mei, H.-Y. (1998) *Biochemistry 37*, 5549−5557.
33. Hermann, T., and Westhof, E. (1999) *J. Med. Chem. 42*, 1250−1261.
34. Luedtke, N. W., Baker, T. J., Goodman, M., and Tor, Y. (2000) *J. Am. Chem. Soc. 122*, 12035−12036.
35. Aboul-ela, F., Karn, J., and Varani, G. (1995) *J. Mol. Biol. 253*, 313−332.
36. Hennig, M., and Williamson, J. R. (2000) *Nucleic Acids Res. 28*, 1585−1593.
37. Hermann, T., and Patel, D. J. (2000) *Science 287*, 820−825.
38. Williamson, J. R. (2000) *Nat. Struct. Biol. 7*, 834−837.
39. Leulliot, N., and Varani, G. (2001) *Biochemistry 40*, 7947−7956.
40. Qin, P. Z., Butcher, S. E., Feigon, J., and Hubbell, W. L. (2001) *Biochemistry 40*, 6929−6936.
41. Dayie, K. T., Brodsky, A. S., and Williamson, J. R. (2002) *J. Mol. Biol. 317*, 263−278.

BI026299A